Extended Abstracts of the 2018 International Conference on Solid State Devices and Materials, Tokyo, 2018, pp279-280

# RF Performance of ALD-$Al_2O_3$ 2DHG Diamond MOSFETs at High Voltage Operation for High Output Power

Shoichiro Imanishi[1], Nobutaka Oi[1], Satoshi Okubo[1], Kiyotaka Horikawa[1], Taisuke Kageura[1], Atsushi Hiraiwa[1] and Hiroshi Kawarada[1,2]

[1] School of Fundamental Science & Engineering Waseda Univ.
3-4-1 Okubo, Shinjuku-ku, Tokyo 169-8555, Japan
Phone: +81-3-5286-3391 E-mail: bz-is-rize@suou.waseda.jp
[2] The Kagami Memorial Laboratory for Materials Science and Technology, Waseda University,
2-8-26 Nishiwaseda, Shinjuku-ku, Tokyo 169-0051, Japan

**Abstract**

**We demonstrate the radio frequency (RF) performance of diamond metal-oxide-semiconductor field-effect transistors (MOSFETs) at high voltage operation (−80 V) for the first time. The MOSFETs with gate length of 0.5 μm and source-gate and gate-drain length of 0.5 and 3.0 μm were fabricated on IIa-type polycrystalline diamond substrate with a (110) preferential surface. At $V_{DS}$ of −80 V, the cutoff frequency $f_T$ and a maximum oscillating frequency $f_{max}$ are 12.1 GHz and 11.5 GHz, respectively.**

## 1. Introduction

Diamond is a promising material for high-power, high-frequency due to excellent semiconductor properties, such as high breakdown electric field, high saturation velocity and high thermal conductivity. We reported the RF performance up to 20 GHz of diamond FETs with 2 dimensional hole gas (2DHG) induced by hydrogen-termination and appropriate adsorbates ahead of the world [1,2]. To date, some excellent cutoff frequency (up to 53 GHz), maximum oscillating frequency (up to 120 GHz) and output power density (up to 2.2 W/mm) of diamond FETs were demonstrated [3-7]. Particularly, the output power density of diamond FETs is higher than that of GaAs and LDMOS [4,6]. However, the operating voltage (~20 V) of these reports is low for diamond because of low breakdown voltage. Output power density would be much more improved by realization of high voltage operation.

On the other hand, we reported high average electric field [8] in MOSFETs with $Al_2O_3$ deposited as gate insulator and [6,9] passivation layer [10] by high temperature atomic layer deposition (ALD) [11].

In this study, we report RF performance of ALD-$Al_2O_3$ 2DHG diamond MOSFETs at high voltage operation ($V_{DS}$ ≦ −80 V) and confirm improvement of RF performance.

## 2. Device Fabrication

The cross-sectional view of the devices is shown in Fig.1. The devices were fabricated [12] on IIa-type polycrystalline diamond substrate with a (110) preferential surface. First, Ti/Pt/Au (20 nm/20 nm/80 nm) were deposited as source and drain electrode and TiC were formed at interface between diamond film and Ti by annealing. Second, the diamond surface was hydrogen-terminated by remote plasma [12]. The isolation was performed by $O_2$ plasma treatment without active area. Third, an $Al_2O_3$ film (100 nm) as gate insulator and passivation layer was deposited by high temperature ALD method (Oxidant: $H_2O$, Temperature: 450 °C) [11]. Finally, Al (100 nm) was deposited as gate electrode. In this work, the source-gate length, gate length, gate-drain length and gate width were 0.5, 0.5, 3.0 and 100 μm, respectively.

## 3. Results and Discussion

Fig.2 shows drain current-voltage ($I_{DS}$-$V_{DS}$) characteristics. Gate voltage ($V_{GS}$) was varied from −20 V to 20 V in steps of 4 V. From Fig.2, the maximum drain current density ($I_{DSmax}$) reached −289 mA/mm at $V_{GS}$ of −20 V and $V_{DS}$ of −40 V. Fig.3 shows $I_{DS}$ and transconductance ($g_m$) dependence on $V_{GS}$. $V_{DS}$ was varied from −40 V to −10 V in steps of 10 V. The maximum transconductance ($g_{mmax}$) was 7.2 mS/mm at $V_{GS}$ of −5.2 V and $V_{DS}$ of −40 V.

Fig.4 shows current gain ($|H_{21}|$) and maximum stable gain (MSG) including parasitic elements (not de-embedded) dependence on frequency. Extrinsic $f_T$ and $f_{max}$ were 12.1 GHz and 11.5 GHz at $V_{GS}$ of 10 V and $V_{DS}$ of −80 V. From this result, high voltage operation was confirmed, thus, the improvement of output power density is expected. To investigate $f_T$ and $f_{max}$ dependence on bias voltage, we evaluated RF performance at different bias voltage. Fig.5 (a) and (b) show extrinsic $f_T$ and $f_{max}$ mapping against $I_{DS}$-$V_{DS}$ characteristics in wide bias voltage (−16 V ≦ $V_{GS}$ ≦ 16 V, −50 V ≦ $V_{DS}$ ≦ 0 V). From Fig.5 (a) and (b), the maximum $f_T$ and $f_{max}$ region is located in the $V_{GS}$ near the threshold voltage and high $V_{DS}$. Total device region reaches near saturation velocity at higher $V_{DS}$. Consequently, improvement of RF performance and output power is expected by high $V_{DS}$ operation.

## 4. Conclusions

We fabricated ALD-$Al_2O_3$ 2DHG diamond MOSFETs and evaluated RF performance at high voltage operation ($V_{DS}$ ≦ −80 V). At $V_{DS}$ of −80 V, $f_T$ of 12.1 GHz and $f_{max}$ of 11.5 GHz were obtained for a 0.5 μm gate-length device without a field plate structure.

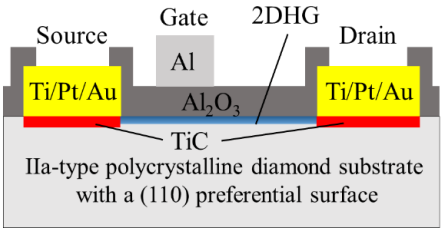


Fig.1 Cross-sectional view of ALD-$Al_2O_3$ 2DHG diamond MOSFETs.

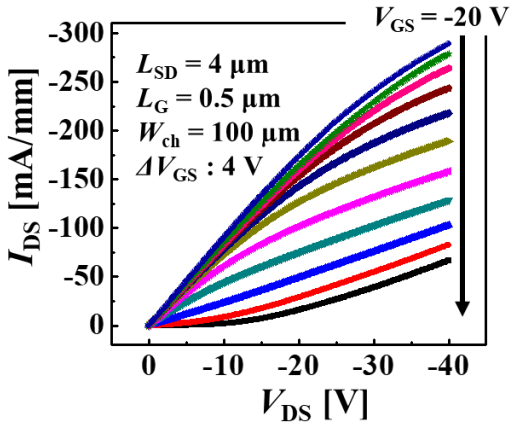


Fig.2 $I_{DS}$–$V_{DS}$ characteristics of ALD-$Al_2O_3$ diamond MOSFET ($L_{SD}$ = 4 μm, $L_G$ = 0.5 μm, $W_{ch}$ = 100 μm). The maximum $I_{DS}$ was 289 mA/mm at $V_{GS}$ = −20 V and $V_{DS}$ = −40 V.

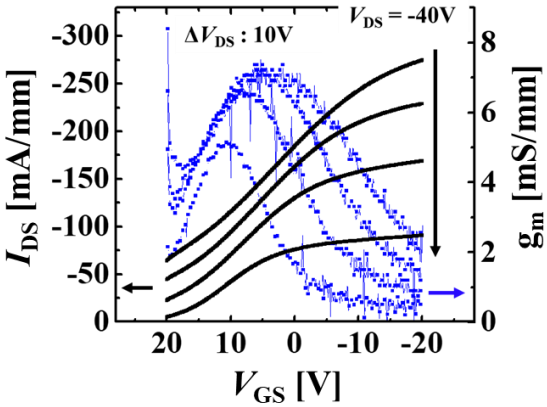


Fig.3 $I_{DS}$-$V_{GS}$ and $g_m$-$V_{GS}$ characteristics of ALD-$Al_2O_3$ diamond MOSFET ($L_{SD}$ = 4 μm, $L_G$ = 0.5 μm, $W_{ch}$ = 100 μm).
The maximum $g_m$ was 7.2 mS/mm at $V_{GS}$ = 5.2 V and $V_{DS}$ = −40 V.

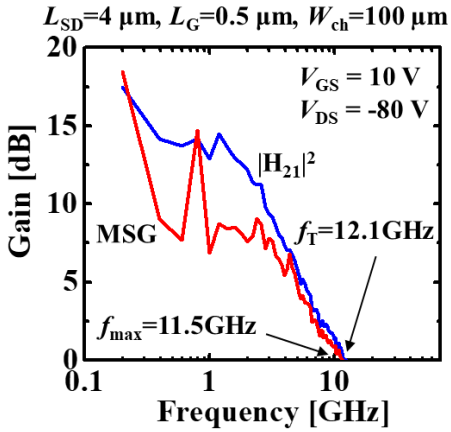


Fig.4 Current gain ($H_{21}$) and maximum stability gain (MSG) as a function of frequency for ALD-$Al_2O_3$ diamond MOSFET ($L_{SD}$ = 4 μm, $L_G$ = 0.5 μm, $W_{ch}$ = 100 μm) at $V_{GS}$ = 10 V and $V_{DS}$ = −80 V.

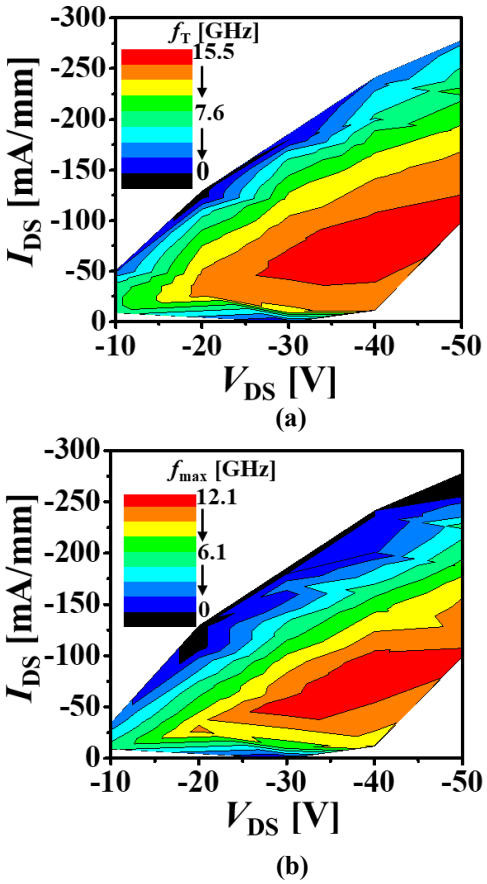


Fig.5 (a) $f_T$ and (b) $f_{max}$ mapping against $I_{DS}$-$V_{DS}$ characteristics in wide bias voltage (−16 V ≦ $V_{GS}$ ≦ 16 V, −50 V ≦ $V_{DS}$ ≦ 0 V).


## Acknowledgements

This study was supported by a Grant-in-Aid for Fundamental Research S (26220903, JSPS). This study was partially supported by Creation of Life Innovation Materials for Interdisciplinary and International Researcher Development.


## References


[1] H. Taniuchi, H. Umezawa, T. Arima, M. Tachiki and H. Kawarada: IEEE Electron Device Lett. 22 (2001) 390.

[2] H. Matsudaira, S. Miyamoto, H. Ishizaka, H. Umezawa and H. Kawarada: IEEE Electron Device Lett. 25 (2004) 480.

[3] M. Kubovic, M. Kasu, I. Kallfass, M. Neuburger, A. Aleksov, G. Koley, M. Spencer and E. Kohn: Diamond and Related Materials **13** (2004) 802.

[4] M. Kasu, K. Ueda, H. Ye, Y. Yamauchi, S. Sasaki and T. Makimoto: Electron. Lett. **41** (2005) 1249.

[5] K. Ueda, M. Kasu, Y. Yamauchi, T. Makimoto, M. Schwitters, D. Twitchen, G. Scarsbrook and S. Coe: IEEE Electron Device Lett. **27** (2006) 570.

[6] K. Hirama, H. Takayanagi, S. Yamauchi, Y. Jingu, H. Umezawa and H. Kawarada: (2007) 873.

[7] S.A. Russell, S. Sharabi, A. Tallaire and D.A. Moran: IEEE Electron Device Lett. **33** (2012) 1471.

[8] H. Kawarada, T. Yamada, D. Xu, H. Tsuboi, Y. Kitabayashi, D. Matsumura, M. Shibata, T. Kudo, M. Inaba and A. Hiraiwa: Scientific Reports **7** (2017) 42368.

[9] M. Kasu, H. Sato and K. Hirama: Applied Physics Express **5** (2012) 025701.

[10] D. Kueck, S. Jooss and E. Kohn: Diamond and Related Materials **18** (2009) 1306.

[11] A. Hiraiwa, A. Daicho, S. Kurihara, Y. Yokoyama and H. Kawarada: J. Appl. Phys. **112** (2012) 124504.

[12] Y. Jingu, K. Hirama and H. Kawarada: IEEE Trans. Electron Devices **57** (2010) 966.